Static and Dynamic Properties of Trapped Cold Fermionic Atoms

Mark DelloStritto

May 20, 2011

Acknowledgements:

I would like to thank the members of my thesis committee, Professor DeSilva, Professor Jang, Professor Venugopalan, and Professor White, for the time and effort they have sacrificed in reviewing my thesis.

I would also like to thank my advisor, Professor DeSilva, who has helped guide me not only in this thesis but in research projects throughout my time at Binghamton. The experiences and opportunities these projects have opened up to me are invaluable and his guidance has been an essential part of my education.

I would like to thank family and friends as well, for it is only through their intangible but important support that I have maintained the spirit necessary to seek a degree in physics.

Abstract

In this paper I derive the static and dynamic properties of two differnt fermionic cold gas system. I derive the thermodynamic properties of a fully polarized noninteracting fermi gas in a quartic trap using a semiclassical approach and a low temperature series expansion method. I also introduce the recently discovered quantity Contact and derive several universal relations associated with it. In order to derive the contact, I use two different methods: a ground-state energy fucntional based on asymptotic limits and Monte Carlo calculations, and BCS Mean Field Theory. I use the universal relations associated with Contact to derive several static and dynamic properties of a balanced strongly interacting gas of fermions with two spin states and large scattering length. The static properties include the total energy, contact density, and polytropic index of the system, and the dynamic properties include the collective oscillations of the trap, the structure factor, and an alternate derivation of the polytropic index. The collective oscillation frequencies are found using both hydrodynamic theory and a sum rule approach and are presented in terms of the contact and homogenous energy. It is found that the static and dynamic properties derived for this system agree well with experimental data and alternative theoretical approaches.

Contents

Chapter 1

Introduction

The field of condensed matter physics is one of the most interesting and exciting fields in physics today. The extreme conditions present in condensed matter make possible the study of novel physics of great interest to theorists. Phenomena such as superconductivity, superfluidity, and the possibility to study macroscopic quantum systems present us with challenges to many accepted models, forcing the development of new models and new physics to explain them. Further, the study of these phenomena has applications to powerful new technologies, such as high temperature superconductors. Finally, there has been such a great interest in this field recently as many new developments in experimental techniques in just the past decade have made it possible to study these systems in the labratory.

Therefore, due to the recent advances in experimental methods, a recent major goal in theoretical physics is to develop models of cold gases which match the flood of experimental data. In this paper I will focus on deriving several properties of two different systems. The first system I will study is a cloud of non-interacting fully polarized fermionic atoms. I will derive the thermodynamic properties of this gas when contained in a quartic potential. The other system I will study is a balanced strongly interacting gas of fermions with two spin states and large scattering length. Recently, Shina Tan was able to derive a quantity associated with these systems deemed Contact ([17],[18],[19]), which is defined as the high momentum tail of the momentum distribution:

$$C = \lim_{k\to\infty} (k^4 n(k)) \tag{1.1}$$

where $n(k)$ is the momentum distribution function. I will connect the Con-

tact with several static and dynamic properties of this system, including the total energy, structure factor, polytropic index, Contact density, and the frequencies of the collective oscillations of the system, and therefore increase the power and scope of the Contact.

Although deriving these properties of the above systems is an interesting theoretical excercise, without experimental data to test our models that is all it will remain. Fortunately however, there have been many recent advancements in the ability to both produce and contol gases at degenerate temperatures well below the fermi temperature. Specifically, advancements in achieving conditions for degeneracy and the use of Feshbach Magnetic resonances have allowed experimentalists to study in great detail systems such as those I investigate in this paper.

This paper is organized as follows: in Chapter 1 I introduce the motivation for study, the general behavior of cold fermi gases, and recent developments for excercising a fine degree of control over these systems. In Chapter 2 I derive the thermodynamic properties of a fully poloraized non-interacting fermi gas at low temperature. In Chapter 3 I introduce Contact, several universal relations associated with the Contact, and the conditions in which these universal relations apply. In Chapter 4 I derive several static and dynamic properties of a balanced strongly interacting gas of fermions with two spin states and large scattering length, including the total energy, structure factor, polytropic index, Contact density, and the frequencies of the collective oscillations of the system. In Chapter 5 I conclude with a summary of this paper and the results derived within.

1.1 Motivation

Cold gas systems display some of the most interesting in physics due to their novel, unique, interesting, and useful properties that can be realized with experimental techniques which allow a great deal of control. There are many properties such as superfluidity, superconductivity, supersolidity, Bose-Einstein condensation, and the fractional quantum hall effect which are observed either only in or primarily in low temperature systems. Further, these phenomena are often counterintuitive, such as a metal that has no resistance to current or a fluid that has no resistance to flow, and thereby challenge our knowlegde of physics and expand its horizon. These systems provide an excellent opportunity to learn and revise current physical law

in order to form a more perfect model of the universe. In addition, these properties often have very powerful future applications, such as electronics with no thermal losses, very accurate atomic clocks, and low temperature models of higher temperature systems.

Another aspect of cold gas systems that is very attractive is the incredible degree of control that can be achieved with relative ease and little equipment. In cold gas systems, the temperature is so low that often the only relevant microscopic variables are the mass, charge, spin, and the interaction between neighboring particles. Unlike higher temperature systems, where emergent properties and chaotic behavior can prevent a direct deterministic interpretation of the system and force a statistical interpretation, all of the aforementioned properties of cold gas systems can be fine tuned to great accuracy. In addition, the growing number of experimental techniques are relatively simple to implement and don't require large, expensive machinery or dangerous matrials.

Finally, cold gas systems are intereting to study as, due to their simple nature and controllability, there is a great deal of freedom in creating new systems. For example, it is possible to model a high temperature superconductor using a well understood low temperature superconductor, create solids that are a million times less dense than air, and build some of the most accurate atomic clocks. The possibilities in cold gas systems are nearly limitless, gauranteeing that there will always be something interesting to study.

The main goals of this project are to increase the power of our theoretical models and the scope of our understanding of the fundamental phsyical principles underlying the behavior of these systems. These goals will only increase the controllability of the systems and allow us to construct a greater number of complex systems and are thus in the spirit of the study of cold gas systems.

1.2 Condensation of Fermions

In order to study phenomena such as superfluidity and superconductivity, it is often necessary to first cool a gas to temperatures at which it becomes fully degenerate, that is, all the particles in the gas occupy the same energy level. This special degenerate state of a gas is known as a Bose-Einstein Condensate, and it was once thought that it could only be achieved with a gas of bosons as the Pauli Exclusion Principle forbids fermions from occupying

the same state. However, it is in fact possible for a gas of fermions to form a BEC in the form of composite bosons, and although not all low temperature phenomena are dependent on the BEC state, it is an important state in low temperature physics. In order to understand how fermions can condense into a BEC, it is first necessary to understand how bosons condense into a BEC.

Bosons behave according to Bose-Einstein statistics, therefore the number of particles in any given energy level is given by the Bose-Einstein destribution: $N_\epsilon = 1/(e^{\epsilon-\mu)/k_B T} - 1)$ where ϵ is the energy of a given level, μ is the chemical potential, k_B is Boltzmann's constant, and T is temperature. At very low temperatures, the number of particles in the ground state is very large and therefore we can use the first two terms of the Taylor expansion of the exponential term in the distribution function. Therefore, the number of particles in the ground state can be written:

$$N_0 = kT/(\epsilon_0 - \mu) \tag{1.2}$$

where ϵ_0 is the ground state energy. If we know the chemical potential, it is then simple to find the temperature at which N_0 is large, however, this is easier said than done.

In order to find the chemical potential, and thereby the critical temperature at which the system of bosons "condenses" into the ground state, it is easiest to begin with the equation $N = \int_0^\infty g(\epsilon)/(e^{\epsilon-\mu)/kT} - 1)$ where $g(\epsilon) \propto \sqrt{\epsilon}$ is the density of states in three dimensions. In order to evaluate this integral, we must first assume that $\mu = 0$, which is a good approximation at low temperatures [15]. The integral gives an equation for the number of particles which is proportional to temperature. This a counterintuitive result as it is implied that this equation can be correct for only one temperature, which we will call the critical temperature: $T_c = N^{2/3}h^2/(2.612 * 2\pi mkV)$.

There is a problem with the integral above as the integrand diverges as ϵ goes to zero. The distribution becomes infinite, however, the density of states goes to zero. The result is that the density of states annihilates the infinite spike of the distribution function at $\epsilon = 0$. This allows the integral to be evaluated, however, it also means that we are not considering the large number of particles in the ground state. Therefore, the equation for the number of particles derived above is valid only for the number of particles in excited states. Rewriting the equation for the number of particles in excited states using the critical temperature and using it to find the equation for the number of particles in the ground state, we find:

$$N_{excited} = (T/T_c)^{3/2}N \tag{1.3}$$

$$N_0 = (1 - (T/T_0)^{3/2})N \tag{1.4}$$

Therefore, below a certain temperature known as the critical temperature a majority of the particles in a system consisting of bosons condense into the ground state. The above mathematical explanation does little to highlight the extrodinary properties of the sytem however, and a qualitative analysis using Heisenberg's Uncertainty Principle is much more effective. At zero temperature, the velocity of all the particles is zero, which implies that the uncertainty in velocity is also zero. Due to the uncertainty principle, the uncertainty in position would then have to be infinite in order for the product of the two uncertainties to be greater than or equal to $\hbar/2$. However, with all the bosons in the same state and the same location in a trap, the uncertainty in position is also near zero. Therefore, in order to have a large enough product of the uncertainties, the wavefunctions of the particles must spread out in space so that the uncertainty in position can be large enough. At a sufficiently low temperature, the wavefunctions spread out so much that the thermal deBroglie wavelength becomes much larger than the interparticle spacing and all of the particles become indistinguishable, leading to macroscopic quantum state with a number of interesting properties.

Even though bosons are required to form a BEC as all the particles in a system must occupy the ground state, fermions in a sense can condense into BEC. This is especially evident if one considers that the first BEC formed was composed of Rubidium atoms, which are themselves collections of fermions. Although the theory of fermions forming a BEC is contained in the much more comprehensive BCS theory, all we need to consider are fermions with attractive interactions. If the attraction between the atoms is strong enough, bound states may form, and if we only consider energy scales which are much lower than the binding energy of the bound state, the bound state can almost always be viewed as a molecule [14, p. 49]. These "Cooper Pairs" can then be considered bosons which can undergo Bose-Einstein condensation. Even when the temperature is not low enough where a majority of particles condense into the same state, these pairs can still exhibit a great deal of degeneracy with interesting consequences, such as superconductivity. Therefore, fermions can in fact behave like bosons in certain situations and

therefore occupy degenerate energy levels, even forming a BEC in the most extreme case.

1.3 Experimental Advancements

In this section I will discuss the techniques employed to achieve degenerate temperatures, to trap cold gases, and to study their properties near the BEC-BCS crossover regime. Specifically, I will discuss the techniques employed to cool matter to sufficiently low temperatures such that all particles occupy the same energy level, both optical and magnetic methods employed to trap a gas, and the use of Magnetic Feshbach Resonances to tune the scattering length and thereby the interaction strength between the particles.

1.3.1 Achieving Degeneracy Temperatures

As discussed above, in order to achieve the degeneracy required to study the most interesting properties of condensed matter we must cool a gas below its critical temperature. However, this is an extremely difficult feat to accomplish as it involves cooling gases from anywhere to a few Kelvin to a millionth of a Kelvin above absolute value. It is not possible to use even liquid helium to achieve these temperatures, and sophisticated techniques are required employing lasers and magnetic fields. Lasers and magnetic fields are also widely employed to trap cold gases, therefore, in this section I will go over techniques to cool and trap gases using lasers and magnetic fields. I will first discuss the trapping of atoms as cooling methods are simply modifications of trapping schemes, and of the trapping schemes I will first discuss magnetic trapping.

In order to understand how atoms are trapped using magnetic fields, we must first understand how the atoms interact with magnetic fields. The interaction of atoms with the magnetic fields is more complicated than with lasers because of the hyperfine splitting of the magnetic energy levels. Assuming that the atoms have zero orbital angular momentum, the hamiltonian describing the magnetic field interaction is given as:

$$H_Z = A\vec{I} \cdot \vec{J} + g\mu_B \vec{B} \cdot \vec{J} \tag{1.5}$$

where I is the nucelar spin angular momentum, J is the electron spin angular momentum, B is the magnetic field, μ_B is the Bohr magneton, g is

the classical spin correction factor, and A is an experimentally determined constant associated with the species of atom [14, p. 6]. The first term is a result of the hyperfine interaction between the nuclear magnetic dipole moment and the magnetic field due to the electrons. The second term is a result of the interaction between the intrinsic magnetic moment of the electrons and the applied magnetic field. It is safe to ignore the interaction between the intrinsic magnetic moment of the nucleus as the ratio between the nuclear magneton and the Bohr magneton is around 1/2000 [14, p. 6].

When one solves the above Hamiltonian to find the dependence of the energy of the system on magnetic field, the following solution is obtained:

$$E = \hbar A((F^2 - I^2 - J^2) + B/B_{hf}) \tag{1.6}$$

where $B_{hf} = A/g\mu_B$. Depending on the constants in the equation and the values of F, I, J, and m_F, its derivative will be either positive or negative. When the slope of the equation is positive, the particles are drawn to lower magnetic field as it offers a state of lower energy. Due to the r^{-2} relationship of the magnetic field, a magnetic field cannot attain a maximum in free space. Therefore, when creating a magnetic trap one must trap atoms in the minimum of a magnetic field. Therefore, we are only interested in those atoms which are "low field seekers," or those where $F = 2, m_F = 2, 1, 0$ and $F = 1, m_F = -1$. These low field seekers will be attracted to the center of the trap, while the "high field seekers" will be attracted to the edge of the trap and will escape from it.

Not all of the low field seekers will remain in the trap indefinitely however, as collisions between atoms can convert low field seekers into high field seekers. There are two states of particular interest that are immune to this effect: the *doubly polarized state* with $F = I + 1/2$, $m_F = F$ and *maximally stretched state* with $F = I - 1/2$, $m_F = -F$.

Most magnetic field traps are axially symmetric, with $\left|\vec{B}\right| = B_0 = \frac{1}{2}\alpha r^2 + \frac{1}{2}\beta z^2$. If the atoms in the trap are moving slow enough, which is a weak assmuption when working with cold gases, it is possible to approximate the system as adiabatic. As the gas behaves adiabatically, the atoms remain in the instantaneous hyperfine Zeeman states corresponding to their current position, despite how the direction of the magnetic field may change [14, p. 10]. It then becomes simple to use an axially symmetric magnetic field to trap a large fraction of a cloud of atoms.

Using optical traps to contain cold gases differs in practice from magnetic

trapping, but it is the same in theory. Optical traps focus lasers on a certain area in order to create a field maximum, which in turn creates a potential minimum if the laser is red-detuned [14, p. 10]. The electric field of the laser polarizes the atoms, which then align themselves opposite the polarizing electric field and thereby seek a potential minimum. There is a concern as to whether the effectiveness of an optical trap depends on the species of atom used. If the detuning is much larger than any spin-orbit splitting, which is a weak assumption, species dependence is negligible [14, p. 10]. Optical traps are useful in that they simplify experiments where the system depends on an external magnetic moment, such as when magnetic feshbach resonances are employed, but have limited applications as the inherent energy of the laser light sets a strict lower limit on the temperature of the gas.

1.3.2 Magnetic Feshbach Resonances

One of the most important parameters of a strongly interacting fermi gas is the scattering length. The scattering length determines the interaction strength of a gas $(k_F a)^{-1}$ and the sign of the scattering length can determine whether a gas lies in the BEC or BCS regimes. However, one of the most important aspects of scattering length is that it diverges at the crossover between the BEC regime, where $a > 0$ and the BCS regime, where $a < 0$. In the extreme limits of forming a BEC or BCS pairs scattering length goes to zero, however, scattering length becomes infinite at the crossover region between those two regimes, as illustrated in Figure 1.1.

As a result, at this crossover region the scattering length must drop out of the equations describing the systems and we reach a regime of universal physics. Results derived at infinite scattering length can be applied to any degenerate system regardless of scattering length, whether it be a cold gas in a labratory or nuetron star matter. Therefore, it is important to be able to control the scattering length of a gas of strongly interacting fermions in order to study sytems at infinite scattering length.

Fine tune adjustment of the interaction between atoms, and thereby the scattering length, of a gas of strongly interacting fermions is achieved through the use of magnetic Feshbach resonances. A Feshbach resonance occurs when the scattering potential of two colliding atoms corresponds to the potential of a weakly bound molecular state. Magnetic Feshbach resonances occur when the spin interacts with an external magnetic field according to the

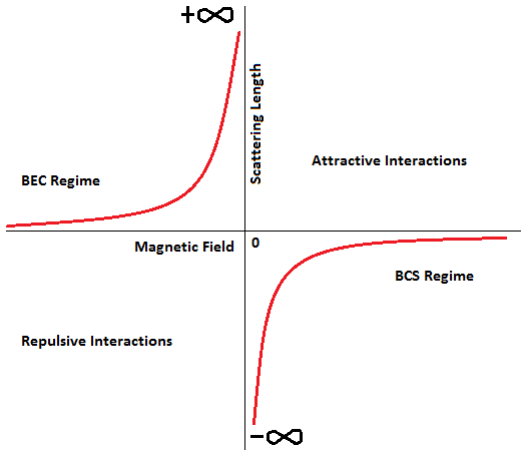

Figure 1.1: Plot of the scattering length of a cold gas with respect to magnetic field value. The scale is arbitrary, with the zero value of magnetic field adjusted to occur at the divergence of scattering length.

hamiltonian:

$$H = \vec{s} \cdot \vec{B} \tag{1.7}$$

. This additional term shifts the interaction potential so that it resonates with a weakly bound dimer state, as illustrated in Figure 1.2:

When the two potential energy curves coincide, a weakly bound dimer state occurs. This dimer is normally very unstable and decays within $100\mu s$ due to the random thermal vibrations of the atoms [20]. However, when the temperature is sufficiently low such that $T/T_f << 1$ (where T_f is the fermi temperature), a dimer state consisting of fermions becomes stable due to Pauli blocking. At such low temperatures, all single atom states which the dimer can decay into are already filled, therefore the Pauli exclusion principle prevents the weakly bound dimer from decaying [4]. It has been found that this process, although only 5% efficient for bosons, is over 50% efficient for fermions [20]. Finally, due to the stability of this bound state and the ability to adjust the interaction due to the interaction of the spin with the magnetic field, it is possible use the magnetic field to tune the interaction between the atoms of the gas. As the interaction between particles is dominated by low energy s-wave sattering, the ability to tune the interaction implies the ability to tune the scattering length as well. Therefore, magnetic Feshbach

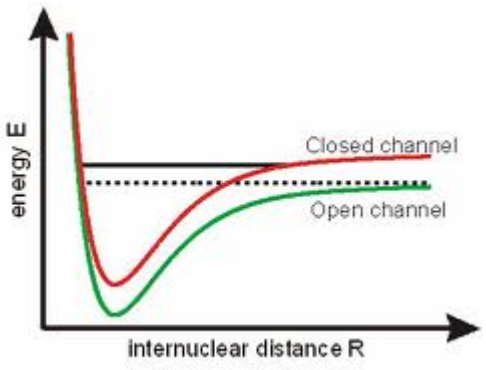

Figure 1.2: Plot of the interaction potential of a dimer versus the internuclear distance. The green curve illustrates the interaction potential under zero magnetic field while the red curve illustrates the interaction potential at Feshbach resonance of the magnetic field. Image courtesy of pit.physik.uni-tuebingen.de

references are a powerful tool which allow experimenters tune the scattering length of a strongly interacting, low energy fermi gas, much like the ones studied in this paper, allowing for experimental validation of our model at the most interesting regime.

Chapter 2

Low Temperature Thermodynamic Properties of a Polarized Fermi Gas in a Quartic Trap

As stated in chapter 1, cold temperature systems are extremely interesting due to the fact that they can display a large number of interesting phenomena while it's also easy to control the systems to a great degree. One of the most interesting phenomena associated with cold gas systems is superfluidity, or the dissapearance of viscosity and resistance to flow at low temperatures. Most superfluid systems are clouds of alkali atoms which have been contained in harmonic optical or magnetic traps.

The equations describing these harmonic traps are dominated by quadratic terms, however, they often include a small quartic term that can have important effects on the dynamics of the gas. It is often desirable to rotate a cold gas system at large values of angular momentum for a number of reasons, including studying the presence of vortices and their effect on superfluidity. However, such systems often become unstable in such regimes due to the centrifugal force. The addition of a positive quartic term to the trapping potential can stabilize these systems at large angular velocity ([6],[3]). In addition, most Guassian optical traps include a small negative quartic term. Therefore, it is desirable to study the effect of a small positive or negative quartic term in the trapping potential on the system.

In order to make this problem tractable, I will assume that the system

is composed entirely of fully polarized non-interacting atoms. This is not difficult to achieve if one traps a single species, or a single hyperfine spin state, of a system composed of fermions. If the system is composed of only one species, the Pauli exclusion principle forbids s-wave scattering, and higher order scattering can be ignored at lower temperatures. Therefore, as all scattering between particles can be ignored, such a system is non-interacting. In addition, as the spin relaxation time for the system is much larger than other experimental time scales, a single species can be maintained for the duration of the experiment. Therefore, it is possible to model the system as a cloud of non-interacting particles obeying Fermi-Dirac statistics confined by potentials given by the equations:

$$V(r,z) = \frac{1}{2}M\omega_r r^2 + \frac{1}{2}M\omega_z z^2 + \gamma r^4 \tag{2.1}$$

$$V(r,z) = br^2 + b_z z^2 + \gamma r^4 \tag{2.2}$$

where M is the mass of the particles, ω_r is the radial trapping frequency, ω_z is the axial trapping frequency, $r^2 = x^2 + y^2$, and γ is the "anharmonic confinement," which determines the strength and sign of the quartic term.

2.1 Derivation of Thermodynamic Variables

As I am studying a system of fermions at low temperature, it obeys Fermi-Dirac statistics, and the average number of particles in a state of energy ϵ_α is given by

$$n_\alpha = \frac{1}{e^{\beta(\epsilon_\alpha - \mu)} + 1} \tag{2.3}$$

where $\beta = 1/k_B T$, k_B is Boltzmann's constant, T is the temperature, and μ is the chemical potential. The average number of particles and the total energy are then given by $N = \sum_\alpha g n_\alpha$ and $U = \sum_\alpha g \epsilon_\alpha n_\alpha$ respectively where g is the spin degenerate factor and is equal to one as the entire system consists of one spin state. If the number of particles is large and the potential energy of the atoms in the trap is much larger than the kinetic energy of the atoms, then the semiclassical Thomas-Fermi approximation can be used. In this approximation, instead of considering energy levels ϵ_α, it is possible to use the phase space single particle energy:

$$\epsilon(r,z,p) = \frac{p^2}{2M} + V(r,z) \tag{2.4}$$

where p is the momentum of a particle and $V(r,z)$ is the potential energy of the particle in the trap. If the number of particles is large, then the fermi energy E_F is large compared to the ground state (not within a few k_BT), the system resembles most room temperature solids, and therefore the semiclassical approximation is possible.

Therefore, using the quantum elementary volume of the single-particle phase space h^3 where h is Planck's constant, the total number of particles in the system can be written as

$$N = \frac{g}{h^3}\int \frac{d^3r d^3p}{Z^{-1}e^{\beta\epsilon(r,p)}+1} \tag{2.5}$$

and the total energy of the system can be written as

$$U = \frac{g}{h^3}\int \frac{\epsilon(r,p) d^3r d^3p}{Z^{-1}e^{\beta\epsilon(r,p)}+1} \tag{2.6}$$

where $Z = e^{\beta\mu}$ and d^3rd^3p is the differential phase space volume. Writing the differential momentum space volume as $d^3p = 4\pi p^2 dp$ and changing variables $\beta p^2/(2M) \to x$, equations 2.5 and 2.6 can be written

$$N = \frac{g}{h^3}\left(\frac{2M\pi}{\beta}\right)^{2/3}\int d^3r f_{3/2}(z_r) \tag{2.7}$$

$$U = \frac{3g}{2h^3}(2M\pi)^{3/2}/\beta^{5/2}\int d^3r f_{5/2}(z_r) + \frac{g}{h^3}\left(\frac{2\pi M}{\beta}\right)^{3/2}\int d^3r V(r,z) f_{3/2}(z_r) \tag{2.8}$$

where $z_r = Z^{-1}e^{\beta V(z,r)}$ and the fermi integral $f_l(z_r)$ is given by

$$f_l(z_r) = \frac{1}{\Gamma(l)}\int_0^\infty \frac{x^{l-1}dx}{z_r^{-1}e^x+1} \tag{2.9}$$

where $\Gamma(l) = \int_0^\infty t^{l-1}e^{-t}dt$ is the gamma function. For low temperatures, or alternatively large values of z_r, it is possible to expand $f_l(z_r)$ as an asymptotic series using a common way method known as Sommerfeld's lemma:

$$f_l(z_r) = \frac{ln(z_r)}{\Gamma(l+1)}[1 + l(l-1)\frac{\pi^2}{6}\frac{1}{ln^2(z_r)} + l(l-1)(l-2)(l-3)\frac{7\pi^2}{360}\frac{1}{ln^4(z_r)} + ...] \tag{2.10}$$

Writing the real space volume element as $\int d^3r = 2\int_0^{z_0} dz \int_0^{r_\perp(z)} 2\pi r_\perp dr_\perp$ where the edges of the cloud are defined as $r_\perp^2 = \sqrt{b^2/(4\gamma^2) + (\mu - b_z z^2)/\gamma} - b/2\gamma$ and $z_0 = \sqrt{\mu/b}$, where b and b_z were defined in equation 2.2, the integrations can be performed analytically in order to obtain expressions for the total number of particles and total energy of the system:

$$N = \frac{g\lambda}{\sqrt{\pi|\tilde{\gamma}|}}[\frac{4}{3\pi}\tilde{\mu}^{5/2} I_{N1}(A) + \frac{\pi^{3/2}}{6}\tilde{\mu}^{1/2}\tilde{T}^2 I_{N2}(A) + O(\tilde{T}^3)] \tag{2.11}$$

$$\tilde{E} = \frac{g}{\sqrt{|\tilde{\gamma}|}}\tilde{\mu}^{7/2} I_{E1}(A) + \frac{g\pi\lambda}{\sqrt{|\tilde{\gamma}|}}\tilde{\mu}^{3/2}\tilde{T}^2 I_{E2}(A) + O(\tilde{T}^3) \tag{2.12}$$

where the dimensionless variables are defined as $\tilde{E} \equiv U/\hbar\omega$, aspect ratio of the harmonic trap $\lambda \equiv \omega_r/\omega_z$, $\tilde{\gamma} \equiv \hbar\mu/(M^2\omega_r^3)$, $\tilde{\mu} \equiv \mu/\hbar\omega_r$, $\tilde{T} = k_B T/(\hbar\omega_r)$, and $A = 1/(16|\tilde{\gamma}\tilde{\mu}|)$. The dimensionless functions $I_{N1}(x)$, $I_{N2}(x)$, $I_{E1}(x) = 4I_{U1}(x)/5 + 4[I_{U3}(x) + I_{U4}(x)]/3$, and $I_{E2}(x) = I_{U2}(x)/2 + [I_{U5}(x) + I_{U6}(x)]/6$ are defined below. The upper sign corresponds to $\gamma > 0$ while the lower sign corresponds to $\gamma < 0$.

$$I_{N1}(x) = \frac{1}{80}(\pm 8(\mp 1 + x)^{5/2}\pi \mp \pi\sqrt{x}(15 \pm 20x \mp 8x^2)) \tag{2.13}$$

$$I_{N2}(x) = \pm\frac{\pi\sqrt{x}}{2} \pm \frac{\sqrt{\pm 1 + \pi x}}{2} \tag{2.14}$$

$$\begin{aligned} I_{U1}(x) = \frac{1}{96}[&\mp\frac{15}{16}\pi\sqrt{x}(8x^2 \pm 16x + 11) \\ &\mp\frac{3}{112}\pi\sqrt{x}(\pm 256x^3 + 616x^2 \pm 560x + 175) \\ &+\frac{48}{7}\pi\frac{x^{9/2} \pm 4x^{7/2} + 6x^{5/2} \pm 4^{3/2} + x^{1/2}}{\sqrt{x(x \pm 1)}}] \end{aligned} \tag{2.15}$$

$$I_{U2}(x) = \frac{1}{4}\left(\frac{2}{3}\pi\frac{x^{5/2} \pm 2x^{3/2} + x^{1/2}}{\sqrt{x(x \pm 1)}} - \frac{1}{3}\pi\sqrt{x}(2x \pm 3)\right) \tag{2.16}$$

$$\begin{aligned} I_{U3}(x) = \frac{1}{280}\pi(&24x^{7/2} - 24x^{3/2}\sqrt{x \pm 1} \pm 56x^{5/2} \\ &\mp 44x^2\sqrt{x \pm 1} + 35x^2 - 16x\sqrt{x \pm 1} \pm 4\sqrt{x \pm 1}) \end{aligned} \tag{2.17}$$

$$I_{U4}(x) = \frac{1}{560}(8\pi(x \pm 1)^{5/2} - \frac{1}{2}\pi\sqrt{x}(16x^3 \pm 56x^2 + 70x \pm 35)) \tag{2.18}$$

$$I_{U5}(x) = \frac{\pi}{6}\frac{-2x^2 + 2x^{3/2}\sqrt{x \pm 1} \mp x + 1}{\sqrt{x \pm 1}} \tag{2.19}$$

$$I_{U6}(x) = \frac{2 \mp 3\sqrt{x(x \pm 1)} \pm 4x - 2x^{3/2}\sqrt{x \pm 1} + 2x^2}{12\sqrt{x \pm 1}} \tag{2.20}$$

Finally, I derive the heat capacity of the system using $C = (\partial U/\partial E)|_N$ and equation 2.12. In order to first obtain a derivative in terms of the correct variables, I write

$$C = \frac{d_B}{\hbar\omega_r}\left(\frac{\partial U}{\partial \tilde{T}}\right)_N \tag{2.21}$$

$$C = \frac{\partial U}{\partial \tilde{T}} + \frac{\partial U}{\partial \tilde{\mu}}\frac{\tilde{\mu}}{\partial \tilde{T}} \tag{2.22}$$

As the number of atoms in the trap is fixed, it safe to assume that $\partial N/\partial\tilde{\mu} = 0$, and therefore

$$C/k_B = \frac{2\gamma\pi\tilde{\mu}^{3/2}}{\sqrt{|\tilde{\gamma}|}}\tilde{T}I_{E2}(A) - \frac{\pi^2}{10}\frac{\tilde{T}}{\tilde{\mu}}\frac{I_{N1}(A)}{I_{N1}(A)}\left(\frac{7g\lambda\tilde{\mu}^{5/2}}{2\pi\sqrt{|\tilde{\gamma}|}}I_{E1}(A) - \frac{g\lambda\tilde{\mu}^{3/2}}{16\pi|\tilde{\mu}|^{3/2}}\right) + O(\tilde{T}^3) \tag{2.23}$$

2.2 Results

Now that I have derived all the relevant thermodynamic properties of the system, it is time to observe their predicted behavior and how well it agrees with physical observation. For these calculations, a large number of atoms on the order of 10^4 is employed in order to ensure the validity of the semi-classical approximation. First I solve equation 2.5 for $\tilde{\mu}$ for given N,T, and λ. As can be seen from figure 2.1, the chemical potential increases with the anharmonic term but decreases with increasing aspect ratio. This makes sense as more energy is needed to excite the fermions in low aspect ratio traps, the chemical potential in low aspect ratio traps is larger than that of higher aspect ratio traps.

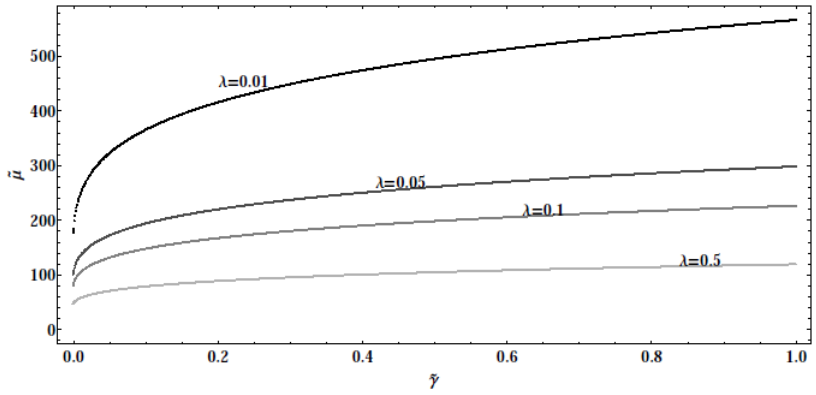

Figure 2.1: Plot of the chemical potential versus the anharmonic term $|\tilde{\gamma}|$ for $N = 10^4$ and temperature $k_BT = \hbar\omega_r$. The different lines are plots for different values of the aspect ratio λ.

If the anharmonic term becomes too negative, the cloud will become unstable as there is no lower limit for the potential energy of the trap. The point at which the anharmonicity dominates over the harmonic confinement is referred to as critical anharmonicity and it depends on the number of atoms in the trap. For a set of representative parameters the critical anharmonicity is plotted as a function of the number of atoms in figure 2.2, and the chemical potential is plotted versus the anharmonic term over a range of negative values in figure 2.3.

In figure 2.4 I plot the total energy as a function of the anharmonic term.

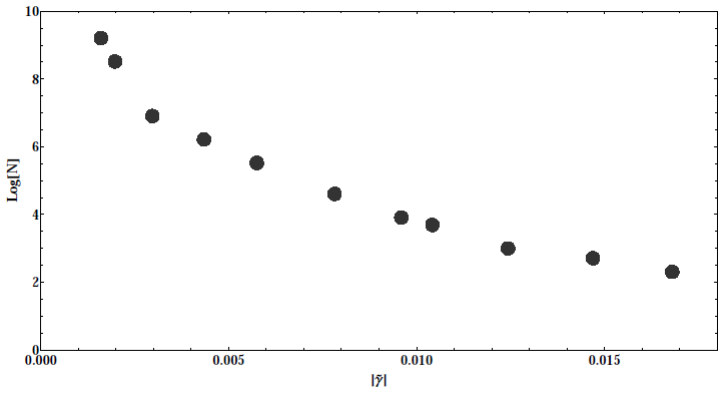

Figure 2.2: A plot of the critical anharmonicity $|\tilde{\gamma}|$ as a function of $Log(N)$. At values of anharmonicity below the critical value, the system becomes unstable. Note that the curve is not perfectly smooth, this is due to numerical noise caused by computational techniques employed to solve for the anharmonicity.

In order to find this quantity, I first calculate the chemical potential from equation 2.11 for a set of representative values for N, T, and λ and then use it to calculate the total energy from equation 2.12. As expected, the total energy increases with an increasing anharmonic term since the trapping potential increases with an increasing anharmonic term.

In figure 2.5 the dimensionless specific heat is plotted versus temperature for several different values of the anharmonic term, in figure 2.6 the dimensionless specific heat is plotted versus temperature for several different values of the aspect ratio, and in figure 2.7 the dimensionless specific heat is plotted verus the anharmonic term. The plots of specific heat with respect to the temperature make sense as we have considered only linear terms in temperature. Meanwhile, the specific heat decreases with incresing anharmonicity which can be seen in equation 2.23.

2.3 Summary

In conclusion, using the semiclassical Thomas-Fermi approximation for a single-species cloud of noninterating fermions I derived expressions for the

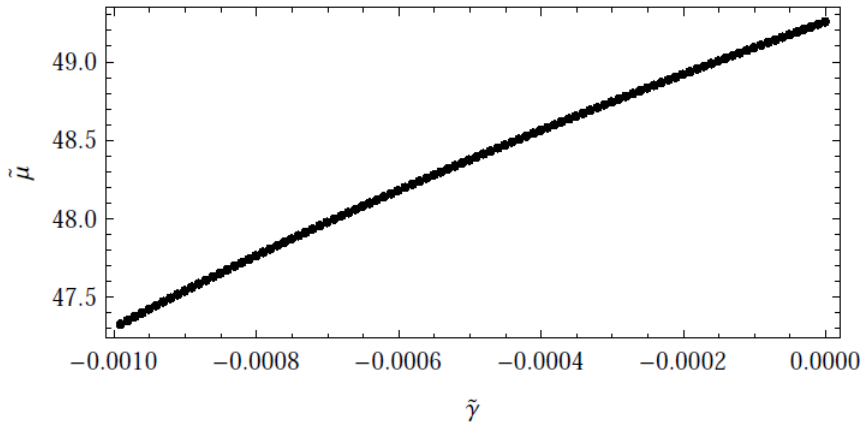

Figure 2.3: Plot of the chemical potential versus negative values of the anharmonic term $|\tilde{\gamma}|$ for $N = 10^4$ and temperature $k_B T = \hbar\omega_r$. For $\tilde{\gamma} < -0.001$, the system is unstable.

total number, total energy, chemical potential, and specific heat of the system in terms of N, T, λ, and γ. I then proceeded to plot the chemical potential, total energy, and specific heat all with respect to the anharmonicity of the system, as well as plotting the specific heat with respect to temperature, and found that they all agree well with the limiting conditions of the system. The calculation of the behavior of these variables for a system contained in a quartic trap is useful due the fact that quartic terms are present in many trapping potentials, including all Gaussian optical potentials, and they can be used to stabilize rapidly rotating gases. Furthermore, even though these calculations involved a very simple system, they form a starting system which can then be altered by adding interaction terms in the future.

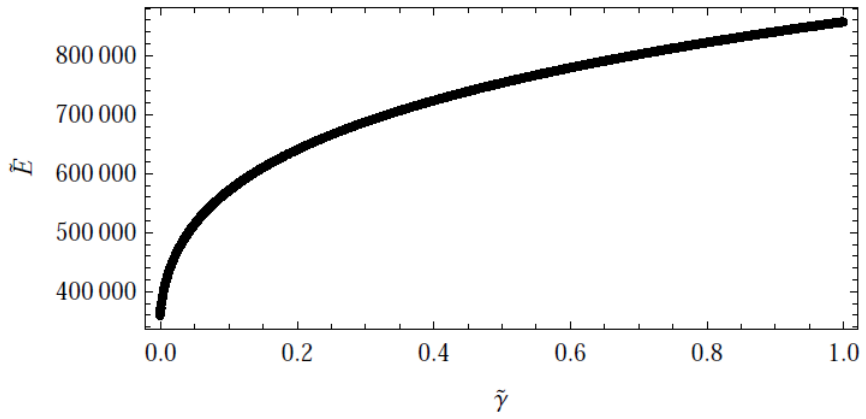

Figure 2.4: Plot of the total energy $\tilde{E}$ versus anharmonicity $|\tilde{\gamma}|$ for $N = 10^4$, temperature $k_B T = \hbar\omega_r$, and aspect ratio $\lambda = 0.5$

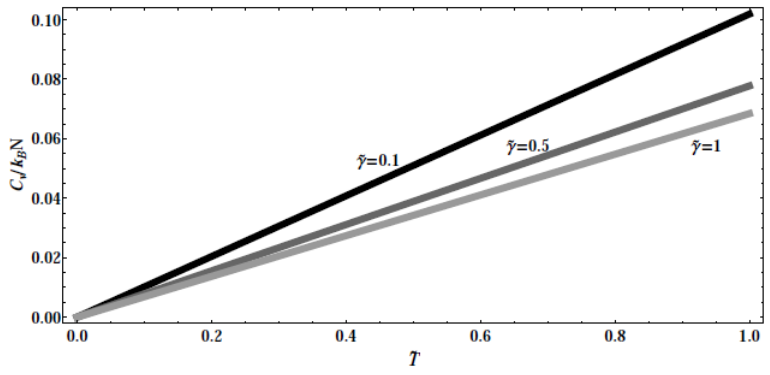

Figure 2.5: Plot of Specific Heat versus temperature with $N = 10^4$ and aspect ratio $\lambda = 0.5$ for different values of the anharmonicity $\tilde{\gamma}$.

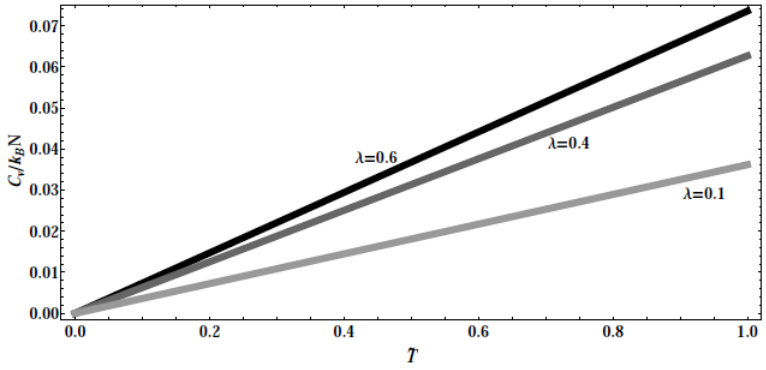

Figure 2.6: Plot of Specific Heat versus temperature with $N = 10^4$ and anharmonicity $\tilde{\gamma} = 0.5$ for different values of the aspect ratio λ.

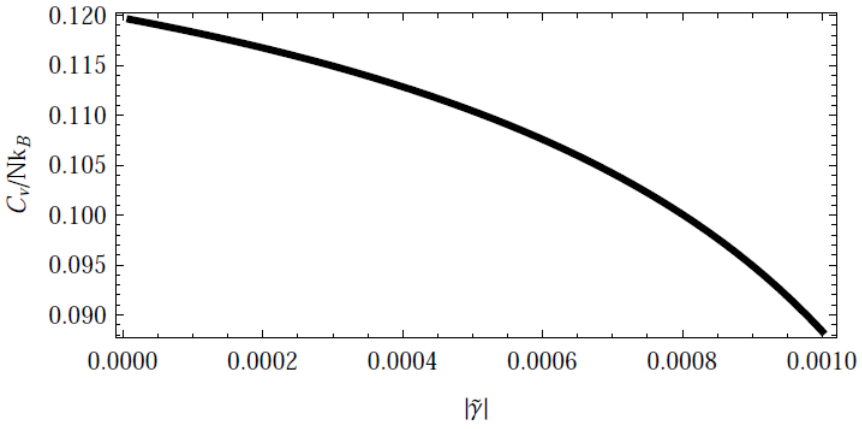

Figure 2.7: Plot of Specific Heat versus the anharmonicity $|\tilde{\gamma}|$ for $\tilde{\gamma} < 0$ with $N = 10^4$ and temperature $k_BT = \hbar\omega_r$.

Chapter 3

Contact

"Contact" is a new quantity recently derived by Shina Tan at Georgia Tech in 2008 which has already promised to be one of the most useful tools for studying the behavior of fermions with two spin states which interact with a large scattering length [2, p. 1]. Contact has already been connected to the momentum distribution and the total energy of appropriate systems, and can be used to derive the derivative of energy with respect to inverse scattering length, to find the sudden change in energy associated with a sudden change in the scattering length, to derive a virial theorem for a system in a harmonic trapping potential, to find the pressure and energy density in a homogenous system, and can be connected to inelastic two-body losses if they exist. In addition, the systems that Contact can be applied to involve strong interactions which can't be treated pertubatively, making the use of Contact one of the few methods of studying these systems. One of the major goals for this project is to further expand the usefulness of Contact by connecting it to the collective oscillations and polytropic index of a gas of strongly interacting fermions in a harmonic trap.

Before we move on with any work on Contact, it is first imperative to understand what Contact is and to what systems it applies to. I will first discuss the systems that Contact can be applied to in order to display the usefulness of Contact and give an understanding as to how it is derived. I will then go over the definition of Contact itself, useful alternative definitions, and applications.

3.1 Systems of Contact

The systems we are most interested in are those that are dominated by short-range interactions that produce a large scattering length, or in other words systems dominated by s-wave scattering. As stated above, due to the strong interactions, these systems are difficult to study as they can't be studied pertubatively with familiar methods, such as Mean Field Theory. Even non-perturbative theories, such as Dynamic Mean Field Theory, are inadequate in describing these strong interactions [2, p. 2]. However, such systems have universal properties that depend only upon the scattering length and upon no other aspect of the system [2, p. 2]. One such system of particular interest is a gas of fermions with only two spin states. It turns out that the number of pairs of fermions with small separations in this system is an important quantity that is intimately connected to the aforementioned universal properties of the system. It is this quantity that is deemed Contact and has become such a useful tool in condensed matter physics.

3.2 Definition of Contact

As stated above, the most basic definition of Contact, although perhaps not the most useful one, is a measure of the number of pairs of fermions with different spins that have small separations (hence the origin of the name "Contact") [2, p. 1]. The most useful definitions of Contact, as well as the source of its utility, come from its universal relations to other properties of the system.

One of the simplest definitions of contact relies on its relationship to the momentum of the system. Contact is related to the momentum distribution $n_\sigma(k)$ for each of the spin states $\sigma = 1, 2$ through the equation

$$C = \lim_{k\to\infty} n_\sigma(k) \cdot k^4 \tag{3.1}$$

where k is the wavevector [2, p. 3]. Thus, Contact can be defined as the high momentum tail of the momentum distribution.

This relation then leads us directly to the relation of Contact to the energy of the system. Recall that it's possible to define the number of particles and kinetic energy of a system as integrals over the momentum density. The problem is that, as the momentum density is proportional to k^{-4} according to the equation 3.1, both quantities are ultraviolet divergent. This implies

that the kinetic energy is sensitive to range, and that the interaction energy of the system must cancel the divergence of the kinetic energy. As we know Contact to be related to the divergence of the momentum density, it can then included in the equation and provides us with a relationship between the energy of a system and the Contact:

$$T + U = \Sigma_\sigma \int \frac{d^3k}{(2\pi)^3} \frac{\hbar^2 k^2}{2m} \left(n_\sigma(\vec{k}) - \frac{C}{k^4} \right) - \frac{\hbar^2}{4\pi m a} C \tag{3.2}$$

In equation 3.2 above, the first term is the kinetic energy, and the second two terms are the interaction energy [2, p. 4]. Notice that, at small values of k, the divergent part of the interaction energy perfectly cancels the divergence of the kinetic energy.

Contact is also related to the density-density correlator of the system and therefore, more importantly for our purposes, the structure factor of the system. Remember that in the most general system where the Contact is applicable, there are two different spin states that the particles can occupy. Therefore, it is possible to define a density-density correlator, which gives the strength of the correlation between the number densities of the two spin states at two points as a function of their separation distance r. This function is a powerful tool as it can give a great deal of insight into the structure of the system as well as serve as a way to find the probability of finding two opposite spin states within a certain volume. The density-density correlator diverges as $1/r^2$ for small separations, and this divergence is proportional to the contact density:

$$\lim_{r \to 0} \left\langle n_1(R + \frac{1}{2}r) n_2(R - \frac{1}{2}r) \right\rangle = \frac{1}{16\pi^2} \left(\frac{1}{r^2} - \frac{2}{ar} \right) C_D(R) \tag{3.3}$$

where $n_1(r)$ is the number density of one spin state, $n_2(r)$ is the number density of the opposite spin state, and C_D is the Contact density, or the number density of pairs of fermions with small separations [2, p. 5]. By taking the Fourier transform of the limit of the density-density correlator (equation 3.3), it is possible to derive a useful corrolary to this relation: the relationship between Contact and the structure factor of the system for high momentum values. The structure factor is an important quantity of a system as it gives insight into the crystal structure of a system, if it is present, and, as it is a measurable quanitity, offers a way to determine the density-density correlator for a system. Taking the Fourier transform, one finds that:

$$\lim_{q\to\infty}(S_{12}(q)) = \frac{1}{8}\left(\frac{1}{q} - \frac{4}{\pi a q^2}\right)C_D \tag{3.4}$$

where q is momentum [2, p. 17]. Therefore, the Contact can also be used to describe the high-momentum tail of the structure factor.

If we restrict our system further, even more useful relations involving Contact can be derived. One important special case is a system in a harmonic trapping potential, for which a Virial Theorem can be derived:

$$T + U - V = -\frac{\hbar^2}{8\pi m a}C \tag{3.5}$$

where T is the kinetic energy, U is the interaction energy, and V is the external potential [2, p. 6]. Even though this is a restriction of our system, and therefore a restriction on the usefulness of the result, a large number of traps employ harmonic trapping potentials, thereby underscoring the importance of this theorem.

A final useful restriction is the assumption of a balanced gas where the two spin states of the gas are equally populated at zero temperature. With this assumption in place, it is possible to derive a relationship between the Contact density and the derivative of the energy density with respect to scattering length, also known as the Adiabatic Sweep Theorem:

$$C_D = \frac{4\pi m a^2}{\hbar^2}\frac{d\epsilon}{da} \tag{3.6}$$

In conclusion, as Tan's relations relate microscopic variables, such as scattering length and momentum, to thermodynamic varibales, such as temperature and the total energy of the gas, they offer powerful theoretical tools that can be used to study cold gases. Of particular interest are strongly interacting balanced fermi gases with large scattering length and two spin states, for it is in these systems that the relationship between Contact and Energy (equation 3.2), Tan's Virial Theorem (equation 3.5), and the relationship between Contact Density and the Energy Derivative (equation 3.6 can be employed.

3.3 Deriving the Contact

3.3.1 The Ground State Energy

One of the most challenging aspects of studying such a strongly interacting system is finding the ground state energy. Unfortunately, there is no analytical solution to this problem, however, it is possible to use numerical simulations along with asymptotic behavior to find a function for the ground state energy of the system. When $a < 0$ at low densities, or when $k_f a << 1$, the ground state energy per particle $\epsilon(n)$ is well approximated by an expansion in the power of $k_f|a|$ [11, p. 1]:

$$\epsilon(n) = 2E_f(\frac{3}{10} - \frac{1}{3\pi}k_f a + 0.055661(k_f|a|)^2 - 0.00914(k_f|a|)^3 + ...) \quad (3.7)$$

where $E_f = \hbar^2 k_f^2/2m$ is the fermi energy and $k_f = (3\pi^2 n)^{1/3}$ is the fermi momentum. In the limit where $a \to -\infty$, $\epsilon(n)$ is proportional to that of the noninteracting fermi gas:

$$\epsilon(n) = \frac{3}{5}E_f(1 + \beta) \quad (3.8)$$

where the universal paramter β is estimated to be $\beta = -0.56$ [11, p. 2]. In the opposite case where $a > 0$ and we are once again in the low density regime, the system redues to the dilute Bose gas of dimers:

$$\epsilon(n) = E_f(-1/(k_f a)^2 + a_m k_f/6\pi + ...) \quad (3.9)$$

where a_m is the boson-boson scattering length a_m[11, p. 3].

Finally, it is possible to use a simple interpolation of the form $\epsilon(n) = E_f P(k_f a)$ to find the ground state energy at any value of scattering length, where $P(k_f a)$ is a smooth function of the interaction strength. The function $P(k_f a)$ for both $a < 0$ and $a > 0$ has been found such that it exactly reproduces Monte Carlo calculations as well as the asymptotic limits. For $a < 0$,

$$P(x) = 3/5 - 2\frac{\sigma_1|x| + \sigma_2 x^2}{1 + \sigma_3|x| + \sigma_4 x^2} \quad (3.10)$$

where $\sigma_1 = 0.106103$, $\sigma_2 = 0.187515$, $\sigma_3 = 2.29188$, and $\sigma_4 = 1.11616$. For $a > 0$,

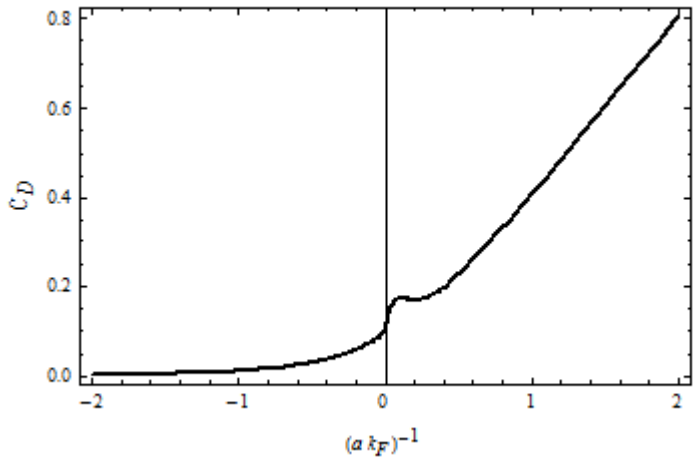

Figure 3.1: Plot of the dimensionless contact density $C_D = C/k_f^4$ with respect to the dimensionless interaction paramter $(k_f a)^{-1}$.

$$P(x) = \frac{E_{mol}}{2E_f} + \frac{\alpha_1 x + \alpha_2 x^2}{1 + \alpha_3 x + \alpha_4 x^2} \tag{3.11}$$

where $\alpha_1 = 0.0316621$, $\alpha_2 = 0.0111816$, $\alpha_3 = 0.200149$, $\alpha_4 = 0.0423545$, and $E_{mol} = -\hbar^2/ma^2$ is the energy of the bound states formed in this regime.

3.3.2 Contact from the Adiabatic Sweep Theorem

Now that we have an expression for the ground state energy of the system, and more importantly the ground state energy per particle, it is now possible to derive the contact density of the system. Recall from equation 3.6 that the contact density is related to the derivative of the ground state energy per particle $\epsilon(n)$ by the scattering length. As $\epsilon(n)$ is different for $a < 0$ and $a > 0$, I had to derive two different expressions for the contact density in these two different regimes. I then checked the asymptotic behavior of these two equations and their derivatives at unitary to ensure that they formed one smooth function when combined.

As can be seen from figure 3.1, and from a more careful analysis of the functions, when placed on the same graph, are indeed continuous as are their

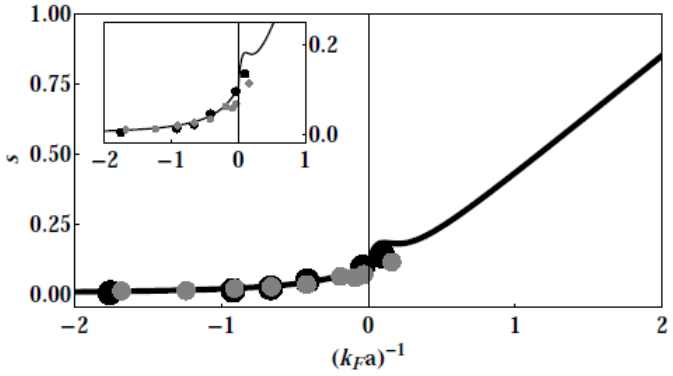

Figure 3.2: Plot of a theoretical calculation of the dimensionless contact density $s = C/k^4$ with respect to the dimensionless interaction parameter $(k_f a)^{-1}$ with experimental data from reference [16] superimposed. The gray circles are results from measurements of the momentum distribution while the black circles are results from radio frequency measurements.

first derivatives. In order to confirm that my calculation of contact is correct it must be compared to experiment. In figure 3.2 is a plot of the dimensionless contact once again with measurements from reference [16].

The data used in figure 3.2 above was taken at a temperature of $T = 0.11T_F$ where T_F is the fermi temperature. The gray circles are results from measurements of the momentum distribution while the black circles are results from radio frequency measurements. As can be seen from the plot above, the theoretical calculation of contact matches measured values quite well for most values in the range. The only discrepancy occurs at $0 < (k_f a)^{-1} << 1$ where there is a sudden and short area of negativity concavity which does not mesh with measured values. This strange "hump" is most likely an artifact resulting from the Pade approximation used to derive the energy functional. As the theoretical calculation of the contact is a zero-temperature model, the experiments were carried out at non-zero temperatures, and the model and data still agree very well, this indicates that the contact is not temperature sensitive for $T << T_F$.

3.3.3 Contact from Mean Field Theory

After Shina Tan was able to derive a number of the universal relations associated with Contact, it was found that they could also be derived within a quantum field theory framework [2, p. 1]. First, I will restrict my analysis to the wide Feshbach resonance in order to avoid the closed channel molecule contribution as it causes problems in the calculation of collective mode frequencies as discussed in section 4.2.2. The fermions which belong to the two different hyperfine states present in the system interact through a short range effective potential $U(r) = g\delta(\vec{r}' - \vec{r})$. The system can then be described by a hamiltonian of the form $H = H_1 + H_2$ where H_1 is the single-particle hamiltonian and H_2 is the interaction hamiltonian.

$$H_1 = \sum_{\sigma} \int d^3\vec{r}\varphi_{\sigma}^{\dagger}(\vec{r})[-\frac{\hbar^2\nabla^2}{2m} - \mu]\varphi_{\sigma}(\vec{r}) \tag{3.12}$$

$$H_2 = -g \int d^3\vec{r}\varphi_{\uparrow}^{\dagger}(\vec{r})\varphi_{\downarrow}^{\dagger}(\vec{r})\varphi_{\downarrow}(\vec{r})\varphi_{\uparrow}(\vec{r}) \tag{3.13}$$

The field operators $\varphi_{\sigma}(\vec{r})$ above obey fermi anticommutation rules and describe the annihilation of a fermion at position $\vec{r}$ in the hyperfine state σ. The arrows $\uparrow$ and $\downarrow$ represent the two different hyperfine states present in the system while m is the mass of the particles and μ is the chemical potential. Using BCS mean field theory decoupling, the ground state grand potential is given by

$$\Omega = \sum_{k} [(\epsilon_k - \mu) - \sqrt{(\epsilon_k - \mu)^2 + \Delta^2}] - \frac{1}{2}\Delta^2\left(\frac{mV}{2\pi\hbar^2 a} - \sum_{k} \frac{1}{\epsilon_k}\right) \tag{3.14}$$

The BCS Bogliubov excitation spectrum of the atoms is given by $E_k = \sqrt{(\epsilon_k - \mu)^2 + \Delta^2}$, where $\epsilon_k = \hbar^2 k^2/2m$ is the kinetic energy and $\Delta = g\left\langle\varphi_{\downarrow}(\vec{r})\varphi_{\uparrow}(\vec{r})\right\rangle$ is the superfluid order paramter. Notice that we have already eliminated the ultraviolet divergences originated from the nature of short-range potential. This was done by regularizing the interaction term according to the relation

$$\frac{m}{4\pi\hbar^2 a} = \frac{1}{g} + \sum_{k} \frac{1}{2\epsilon_k} \tag{3.15}$$

The gap equation is obtained by the minimization of the grand potential density with respect to the superfluid order paramter:

$$-\frac{m}{2\pi\hbar^2 a} = \frac{1}{V}\sum_k \left(\frac{1}{\sqrt{(\epsilon_k - \mu)^2 + \Delta^2}} - \frac{1}{\epsilon_k}\right) \tag{3.16}$$

The fermions number density $n = N/V$ is obtained by the variation of the grand potential density with respect to the chemical potential

$$n = \frac{1}{V}\sum_k \left(1 - \frac{\epsilon_k - \mu}{\sqrt{(\epsilon_k - \mu)^2 + \Delta^2}}\right) \tag{3.17}$$

Finally, evaluating $\partial\Delta/\partial a$ from the gap equation, we find the contact density

$$C_D = \frac{4\pi m a^2}{\hbar^2}\left(\frac{\partial\Omega}{\partial a}\right)_{\mu,T} = \frac{m^2}{\hbar^4}\Delta^2 \tag{3.18}$$

By converting the sum into an integral over momentum, we numerically solve both the gap equation and the number equation simultaneously to find the superfluid order paramter Δ. In figure 3.3, the black line is the dimensionless contact density from mean field theory, the gray line is the dimensionless contact density derived from the energy functional method, and the inset shows experimental data from reference [16]. As can be seen, the results from the two different methods of derivation agree very well with each other and with experimental data, the only error being the "bump" due to the artifact from the Pade approximation used to derive the energy functional.

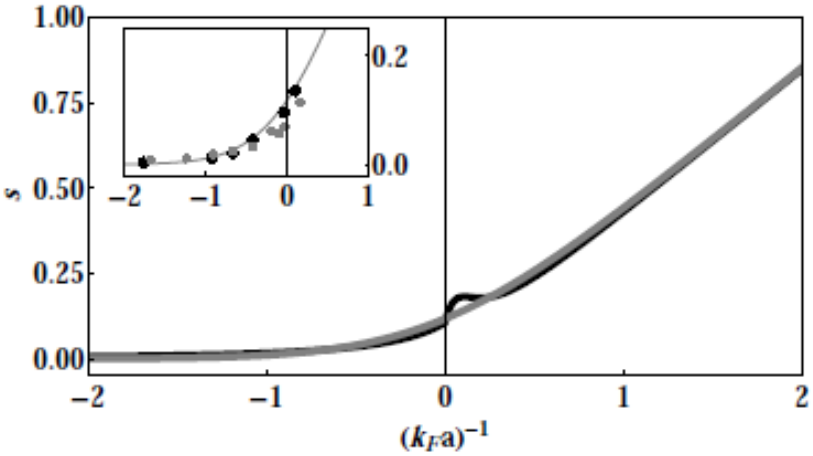

Figure 3.3: A plot of the dimensionless contact density $s = C/k_f^4$ with respect to the dimensionless interaction strength $(k_f a)^{-1}$ as derived from mean field theory, the black line, and as derived from the adiabatic sweep theorem, the gray line, with experimental data from [16].

Chapter 4

Statics and Dynamics of a Balanced Strongly Interacting System of Fermions with Large Scattering Length

One of the main goals of my project is to increase the usefullness and scope of the already powerful Contact by connecting to the statics and dynamics of a balanced, strongly interacting fermi gas with two spin states and large scattering length. The conditions of this system allow us to use Tan's contact as well as several associated universal relations, including the adiabatic sweep theorem (equation 3.6), the virial theorem (equation 4.27), and Tan's Virial Theorem (equation 3.5). Using these and other universal relations along with hydrodynamic theory, I will derive both static and dynamic properties of this system in a harmonic trap. The static properties will include the total energy, contact density, and polytropic index of the system, and the dynamic properties will include the collective oscillations of the trap, the structure factor, and an alternative derivation of the polytropic index. Note that although the polytropic index and structure factor are not necessarily "dynamic" properties of a system, they are derived alongside the collective oscillations of the system, and are therefore included in the section on dynamic properties.

4.1 Static Properties of Trapped Systems

In this section my main goal will be to derive the energy density and contact density of our trapped system, however, in order to do so I must first derive a formula for the polytropic index. Therefore, this section is divided into a derivation of the polytropic index followed by a derivation of the total energy and contact density.

4.1.1 Polytropic Index

The polytropic index is related to the chemical potential of our gas by the relation

$$\gamma = \frac{n}{\mu}\frac{\partial \mu}{\partial n} \tag{4.1}$$

where n is the number density of the system and μ is the chemical potential of the system. In order to find the polytropic index, we must first find an expression for the chemical potential, which is accomplished using the Gibbs-Duhem relation:

$$\mu = \frac{\partial(n\epsilon(z))}{\partial n} \tag{4.2}$$

where $z = (k_F a)^{-1}$ and $\epsilon(z)$ is the ground state energy. Using this relation, I found that

$$\mu_{BCS} = \frac{5}{3}P_{BCS}(z^{-1}) + \frac{\pi}{2}\epsilon_F C_d z^{-1} \tag{4.3}$$

where μ_{BCS} is the chemical potential in the regime where $a < 0$ and $P_{BEC}(z)$ is the function 3.10 multiplied by ϵ_F to give the energy functional for the system. Similarly, I found that

$$\mu_{BEC} = \frac{5}{3}P_{BEC}(z^{-1}) + \frac{\pi}{2}\epsilon_F C_d z^{-1} \tag{4.4}$$

where μ_{BEC} is the chemical potential in the regime where $a > 0$ and $P_{BCS}(z)$ is the function 3.11 multiplied by ϵ_F to give the energy functional for the system. For the case where $a > 0$ I once again ignored the contribution of the molecular bond state $E_{mol} = \frac{-\hbar^2}{ma^2}$ because it was not included in the calculation of the binding energies. For both expressions of μ above, I find that the polytropic is given by the expression:

$$\gamma = \frac{10P_{BCS/BEC}(z^{-1})/3 + 3\pi C_D z^{-1} + \pi\partial S/\partial/2z^{-1}}{5P_{BCS/BEC}(z^{-1}) + 3\pi C_D z^{-1}/2} \tag{4.5}$$

where $P_{BCS/BEC}(z^{-1})$ is the appropriate function for the regime in which we are working.

4.1.2 Total Energy and Contact Density of a Trapped System

In order to derive both the total energy and the contact density of our system, it is necessary to use both local density approximation and the polytropic index. Within the local density approximation the inhmogeneity of the system is taken into account by using the spatially varying chemical potential $\mu = \mu_0 - m\omega_0^2 r^2/2$ where ω_0 and μ_0 are the trapping frequency and the chemical potential at the center of the trap. As $\mu \propto n^\gamma$ where n is the number density of the system, we can assume that $\mu = An^\gamma$ where A is an arbitrary constant [5]. Beginning with the equation $N = \int d^3\vec{r}n(r)$ along with equation for μ we just defined, it is possible to write

$$N = \frac{4\sqrt{2}\pi}{A^{1/\gamma}(m\omega^2)^{3/2}} \int_{-\infty}^{\mu_0} \mu^\gamma \sqrt{\mu_0 - \mu} d\mu \tag{4.6}$$

Similarly, using the equation for the kinetic and interaction energies $E = T + U = \int d^3\vec{r}\epsilon(r)$, where $\epsilon(r)$ is the energy at density at position r, along with our definition of μ, it is possible to write

$$E = \frac{8\sqrt{2}\pi}{3A^{1/\gamma}\gamma(m\omega^2)^{3/2}} \int_{-\infty}^{\mu_0} \mu^{1/\gamma}(\mu_0 - \mu)^{3/2} d\mu \tag{4.7}$$

Finally, using this same method and the expression for the trapping potential $V = \frac{1}{2}m\omega_0^2 \int d^3\vec{r}r^2 n(r)$ it is possible to write

$$V = \frac{4\sqrt{2}\pi}{A^{1/\gamma}(m\omega^2)^{3/2}} \int_{-\infty}^{\mu_0} \mu^\gamma (\mu_0 - \mu)^{3/2} d\mu \tag{4.8}$$

Combining all of these equations, one finds that $E = \frac{2}{3\gamma}V$. Combining this with the expression for the total energy $E_T = T + U + V$ one finds an expression for the total energy density

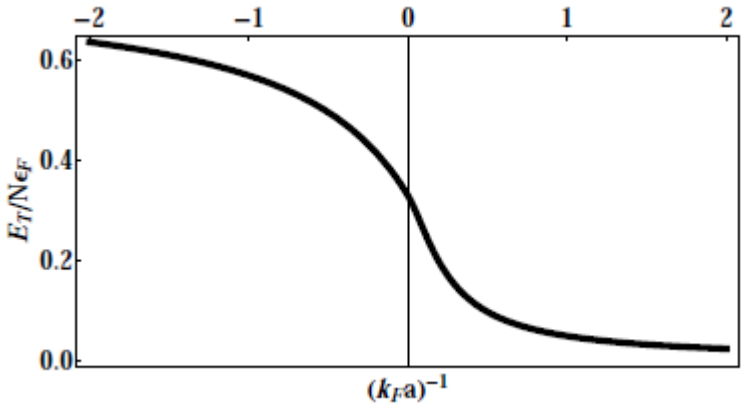

Figure 4.1: A plot of the ratio between the total energy and the number of particles of our system E_T/N with respect to the dimensionless interaction strength $(k_Fa)^{-1}$

$$\frac{E_T}{N} = \frac{2+3\gamma}{3\gamma} \frac{\int_{-\infty}^{\mu_0} \mu^\gamma (\mu_0 - \mu)^{3/2} d\mu}{\int_{-\infty}^{\mu_0} \mu^\gamma \sqrt{\mu_0 - \mu} d\mu} \tag{4.9}$$

The total energy divided by the number of particles is plotted with respect to the dimensionless interaction strength $(k_Fa)^{-1}$ in figure 4.1. Finally, if this result is combined with Tan's Virial Theorem, equation 3.5, on can obtain an equation for the ratio of contact density of our system to the dimensionless interaction strength:

$$C_D/(k_Fa) = \frac{4E_T}{3\pi N\epsilon_F} \frac{2-3\gamma}{2+3\gamma} \tag{4.10}$$

This quantity is plotted versus dimensionless interaction strength in figure 4.2 with the filled circles representing experimental data from reference [16].

4.2 Dynamic Properties of Trapped Systems

4.2.1 Hydrodynamic Theory

Although it is a goal of this project to connect the Contact to the frequencies of the collective oscillations of the system under consideration, it is possible

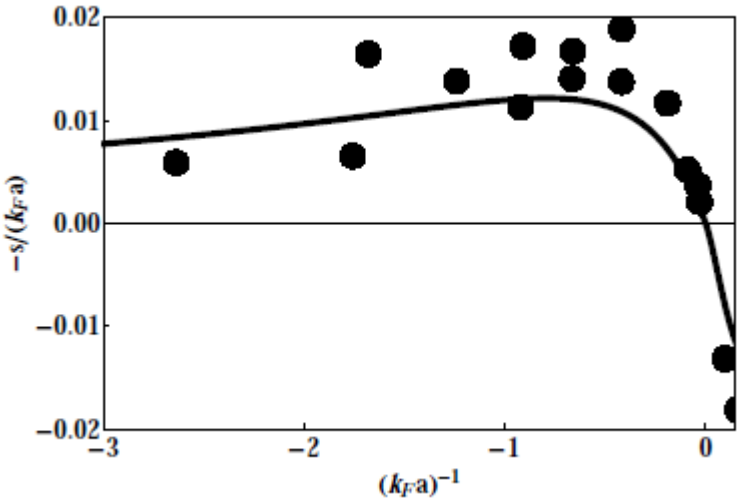

Figure 4.2: A plot of the ratio between the dimensionless contact and the dimensionless interaction strength of our system $s/(k_F a)$ where $s = C_D/k_F^4$ with respect to dimensionless interaction strength $(k_F a)^{-1}$ with experimental data from [16]

to derive these frequencies using hydrodynamic theory. There are several advantages to this approach, including providing an independent test of the monopole and quadrupole frequencies for a spherically symmetric trap, providing a method to determine the radial and axial monopole frequencies for an axially symmetric trap, and providing a method to find an expression for the polytropic index.

The dynamics of the gas can be described using the time-dependent, nonlinear Schrodinger equation, also known as the Gross-Pitaevskii equation:

$$i\hbar\varphi(r,t) = [\frac{\hbar^2}{2m}\nabla^2 + V(r) + \mu(n(r,t))]\varphi(r,t) \tag{4.11}$$

where $\varphi(r,t) = \sqrt{n(r,t)}exp(i\phi(r,t))$ is the superfluid wavefuntion. Equation 4.11 can be converted into a continuity equation and an Euler equation,

$$\frac{dn}{dt} = -\nabla \cdot [n(r,t)\vec{v}] \tag{4.12}$$

and

$$m\frac{dv}{dt} = -\nabla[\frac{1}{2}m\vec{v}^2 + V(r) + \mu(n) + qp] \tag{4.13}$$

respectively, where $qp = (-\hbar^2\nabla^2\sqrt{n})/(2m\sqrt{n})$ is the quantum pressure term. In the Thomas-Fermi approximation I assume that the gas is locally uniform so that this term can be ignored. This Thomas-Fermi regime can be realized in the thermodynamic limit where N/V is constant. It is interesting to note that once I drop the quantum pressure term these equations are classical so that these hydrodynamic equations are applicable for both Fermi and Bose superfluids. However, the hydrodynamic equations are sensitive to quantum corrections, statistics, and dimensionality through the equation of state which enters through the density dependent local chemical potential $\mu(n)$. This hydrodynamic description is valid as long as the collisional relaxation time is much smaller than the inverse of the collective oscillation frequencies.

For the ground state case, $n(r,t) = n_0(r)$ and $v(r,t) = 0$. In order to study the collective oscillations above the ground state, I linearize the hydrodynamic equations by writing $n(r,t) = n_0(r) + \delta n(r,t)$ and $v(r,t) = \delta v(r,t)$. After neglecting the higher order terms and keeping only the linear terms and then by combining the continuity and Euler equations, one finds the linearized version of the hydrodynamic theory:

$$\frac{\partial^2 \delta n}{\partial t^2} = \nabla \cdot [\frac{n_0}{m} \nabla \frac{\partial \mu}{\partial n} \delta n] \tag{4.14}$$

Taking $\delta n(r,t) = \delta n(r) exp[i\omega t]$ and $\mu = An^\gamma$ where A is an arbitrary constant and γ is the polytropic index, equation 4.14 can be converted into a linear eigenvalue problem. In the Thomas-Fermi regime, the continuity and Euler equations admit the ground state density $n_0(r) = n_0(1 - r^2/R_{TF}^2)^{1/\gamma}$ where the Thomas-Fermi radius is given by $R_{TF} = \sqrt{2An_0/(m\omega_0^2)}$. Rescaling the length, density, and oscillation frequency by introducing $\tilde{r} = r/R_{TF}, \tilde{n}_0(\tilde{r}) = n_0(r)/n_0(0)$, and $\tilde{\omega} = \omega/\omega_0$ respectively, equation 4.14 can be written in dimensionless form:

$$\frac{2\tilde{\omega}^2}{\gamma} \delta n = \tilde{\nabla} \cdot [\tilde{n}_0 \tilde{\nabla} \tilde{n}_0^{\gamma-1} \delta n] \tag{4.15}$$

For a spherically symmetric trap, the angular momentum l and its projection onto the z-axis m are good quantum numbers. Following the approach in references [9] and [21], the solution for the density fluctuations has the form $\delta n = R(\tilde{r}) Y_{lm}(\theta, \phi)$, where $R(\tilde{r}) = \tilde{r}^l \tilde{n}_0^{\gamma-1} (1 - \tilde{r})^{1/(\gamma-1)} f(\tilde{r})$. The function $f(\tilde{(r)})$ satisfies the hypergeometric differential equation,

$$\tilde{r}(1 - \tilde{r}) \frac{\partial^2 f}{\partial \tilde{r}^2} + [l + 3/2 - (l + 3/2 + 1/\gamma)\tilde{r}] \frac{\partial f}{\partial \tilde{r}} + \frac{\omega^2 - l}{2\gamma} f = 0 \tag{4.16}$$

The solutions of this differential equation are hypergeometrical functions ([9],[21]) and the eigenvalues are given by

$$\tilde{\omega}_{lm}^2 = l + n_r \gamma (2n_r + 2l + 1) + 2nr \tag{4.17}$$

with radial quantum number $n_r = 0, 1, 2, ...$ and angular momentum quantum number $l = 0, 1, 2, ...$ The monopole mode frequency, or the breathing mode frequency, for a spherically symmetric trap occurs at $n_r = 1$ and $l = 0$, and is given by

$$\omega_M = \sqrt{3\gamma + 2} \tag{4.18}$$

This model predicts that at the weakly repulsive BEC limit $\omega_M = 2\omega_0$ and $\omega_Q = 2\omega_0$, and at the weakly coupling BCS limite $\omega_M = \sqrt{5}\omega_0$ and $\omega_Q = \sqrt{2}\omega_0$. At unitarity where $a = 0$, universality requires that $\omega_M = \omega_Q = 2\omega_0$.

4.2.2 Contact, Collective Oscillations, the Polytropic Index, and the Structure Factor

As we are analyzing the collective oscillations of a cloud of atoms, linear response theory provides an excellent tool with which to study the system. As the oscillations of the cloud must be very small with respect to the cloud's diameter in that dimension in order for the trap to remain stable, the perturbation of the system is weak. In addition, as the cloud is isolated in a magnetic trap, the introduction and elimination of collective oscillations occurs adiabatically. Therefore the excitation operator on the system is linear to a good approximation [7, p. 2]. The response function $\chi(z)$ of the complex frequency z can then be written in terms of the second derivative of the response function [10, p. 23]:

$$\chi(z) = \int \frac{d\omega}{\pi} \frac{\chi''(z)}{\omega - z} \tag{4.19}$$

If you expand the response function in terms of $1/z$, the moment of the expansion of $\chi(z)$ is given by the equation:

$$\chi(z) = \sum_p \frac{1}{z^p} m_{p-1} \tag{4.20}$$

where the p^{th} moment is defined as

$$m_p = \int \frac{d\omega}{\pi} \omega^p \chi''(z) \tag{4.21}$$

Therefore, in order to find the p^{th} moment one must calculate the response function associated with the mode excitation operator. One way to find the moments without calculating the response function is the sum rule approach. The usefulness of this approach is obvious, it is not necessary to know the response function for the collective modes in order to carry out calculations of the frequencies. However, this approach also has a disadvantage as it only provides rigorous upper bounds to the lowest collective mode frequency excited by the excitation operator. If the system is highly collective though, that is the entire cloud oscillates at one frequency and thereby the response function is almost exhausted by a single mode, then the sum rule approach gives the exact collective mode frequency. The excitation energies are given by either m_{p+1}/m_p or $\sqrt{m_{p+2}/m_p}$. I estimate the excitation energies of the collective modes using the ratio:

$$\hbar\omega = \sqrt{m_3/m_1} \tag{4.22}$$

Using the completeness relations, the moments can be written as:

$$m_1 = \frac{1}{2}\left\langle [Q^t, [H, Q]] \right\rangle \tag{4.23}$$

$$m_3 = \frac{1}{2}\left\langle [[Q^t, H], [[H, [H, Q]]]] \right\rangle \tag{4.24}$$

where Q is the mode excitation operator and H is the Hamiltonian of the system.

$$H = \sum_i (\frac{p_i^2}{2m} + \frac{1}{2}\sum_\alpha m\omega_\alpha^2 r_{i\alpha}^2) + g\sum_{i\uparrow j\downarrow} \delta(\vec{r_i} - \vec{r_j}) \tag{4.25}$$

$$H = \sum_\alpha (T_\alpha + V_\alpha) + U \tag{4.26}$$

where $\alpha = x, y, z$. Using the equation of motion of the operator $Q \equiv Q_\alpha = \sum_i r_{i\alpha}^2$, one finds that $\dot{Q_\alpha} = [Q_\alpha, H]/(i\hbar) = \sum_i (r_{i\alpha}p_{i\alpha} + p_{i\alpha}r_{i\alpha})/m$ and $\ddot{Q_\alpha} = 4(T_\alpha - V_\alpha + U/2)/m$. In equilibrium Q_α is time independent, therefore $\ddot{Q_\alpha} = 0$. Then summing over all three components, this follows the virial theorem:

$$2T - 2V + 3U = 0 \tag{4.27}$$

For a spherically harmonic oscillator potential with $\omega_\alpha = \omega_0$ for all α, the three terms represent the kinetic energy $T = \langle \sum_i p_i^2/(2m) \rangle$, the harmonic oscillator potential energy $V = m\omega_0^2 \int \vec{r}^2 n(r) d^3r/2$, and the average mean-field interaction energy $U = g\int n^2(r) d^3r/4$ where $n(r)$ is the total density of the atoms in the trap.

The excitation operators corresponding to the dipole, monopole, and quadropole modes are $Q = \sum_i z_i, Q = \sum_i \vec{r}_i^2$, and $Q = \sum_i (\vec{r}_i^2 - 3z_i^2)$ respectively. By evaluating the commutators in equations 4.23 and 4.24, the collective mode frequencies for the dipole, monopole, and quadropole modes are

$$\omega_D = \omega_0 \tag{4.28}$$

$$\omega_M = 2\omega_0\sqrt{\frac{T+3V+3U}{2Nm\omega_0\left\langle\vec{r}^2\right\rangle}} \tag{4.29}$$

$$\omega_Q = 2\omega_0\sqrt{\frac{T+V}{4Nm\omega_0\left\langle\vec{r}^2\right\rangle}} \tag{4.30}$$

By combining the virial theorem in equation 4.27 and Tan's Virial theorem in equation 3.5 derived in section 3.2, it is possible to express the monopole and quadropole mode frequencies in terms of the energy density and Contact density.

$$\omega_M = 2\omega_0\sqrt{1+A} \tag{4.31}$$

$$\omega_Q = 2\omega_0\sqrt{1-2A} \tag{4.32}$$

where

$$A = \frac{3}{4}\frac{2}{1+8\pi ma\epsilon/(\hbar^2 C_D)} \tag{4.33}$$

where ϵ is the homogenous energy density and C_D is the Contact density. In the BEC regime it is possible for bound states to form, with an energy E_{mol} included in equation 3.11, however, I ignored this term in my calculation of the collective mode frequencies in the BCS regime as the molecular energy was not included in the calculation of the binding energy and thus leads to infinities in the asymptotic behavior of the frequencies. Note however that in the BEC regime $\epsilon' = \epsilon - E_{mol}$ and $C_D' = C_D - 4k_F^4/(3\pi k_F a)$. Also note that these upper bounds are universal as it is not required that one know the exact form of the harmonic potential in order to calculate the collective mode frequencies. Further, the many body and temperature effects are incorporated in the Contact density and homogenous energy density.

In Figure 4.4 the dimensionless monopole and quadrupole collective mode frequencies, ω_M/ω_0 and ω_Q/ω_0 respectively, for a spherical trap are plotted with respect to the dimensionless interaction strength $(k_F a)^{-1}$. At unitarity, the two different plots and their derivatives for $a > 0$ and $a < 0$ have the same value for both cases, thus the functions are smooth for all values of a. At unitarity $\omega_M = \omega_Q = 2\omega 0$, in the weakly repulsive BEC limit $\omega_M = 2\omega_0$ and $\omega_Q = 2\omega_0$, and in the weakly coupling BCS limit $\omega_M = \sqrt{5}\omega_0$ and

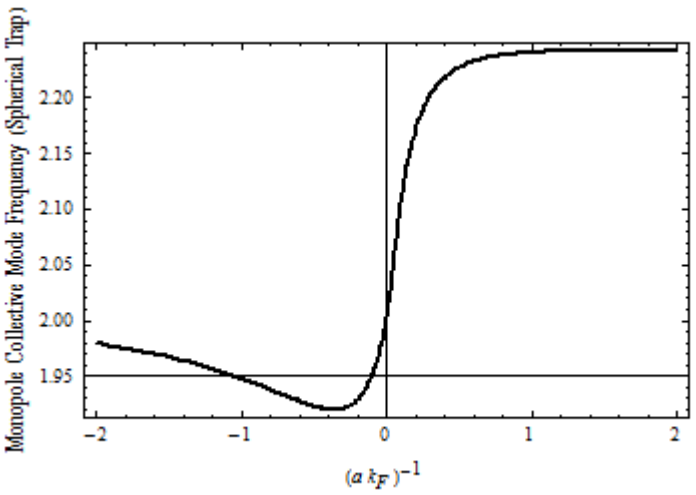

Figure 4.3: The plot of the dimensionless monopole collective frequency for a spherical trap ω_M/ω_0 versus the dimensionless interaction strength $(k_F a)^{-1}$.

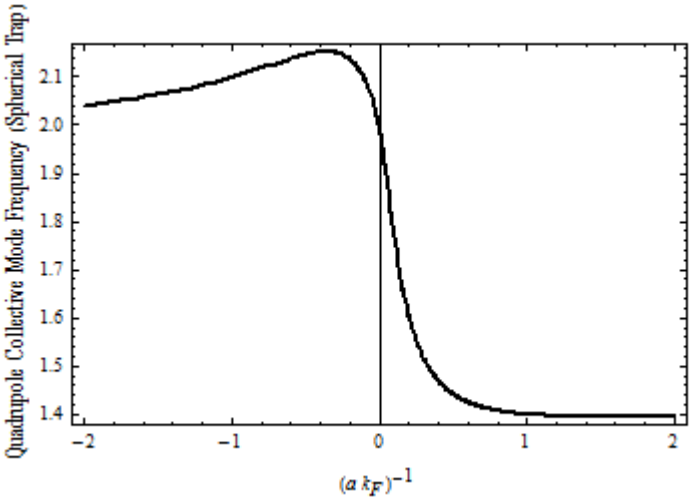

Figure 4.4: The plot of the dimensionless quadrupole collective frequency for a spherical trap ω_Q/ω_0 versus the dimensionless interaction strength $(k_F a)^{-1}$.

$\omega_Q = \sqrt{2}\omega_0$, which are all consistent with the results from hydrodynamic theory derived in section 4.2.1.

In order to find the axial and radial monopole mode frequencies for an axially symmetric trap with potential $V(r) = \frac{m}{2}(\omega_r(x^2+y^2) + \omega_z z^2)$, it is necessary to generalize hydrodynamic theory to such a trap. Doing so, one finds that the lowest frequency axial and radial monopole frequencies are $\omega_a = \omega_z\sqrt{3-(\gamma+1)^{-1}}$ and $\omega_+ = \omega_r\sqrt{2(\gamma+1)}$ respectively [9],[22]. These expressions are only valid for $\lambda \equiv \omega_z/\omega_r << 1$, however, experimental results are only available for this case anyway [12],[1]. For the limiting cases where $\gamma = 1$ and $\gamma = 2/3$ the axial mode frequencies are $\omega_a = \sqrt{5/2}\omega_z$ and $\omega_a = \sqrt{12/5}\omega_z$ and the radial mode frequencies are $\omega_+ = 2\omega_r$ and $\omega_+ = \sqrt{10/3}\omega_+$, respectively. The plots of the dimensionless axial and radial monopole collective mode frequencies, ω_a/ω_z and ω_+/ω_r respectively, versus the dimensionless interaction strength $(k_F a)^{-1}$ are included in Figure 4.6.

The polytropic index is an important quantity as it relates the pressure and density of the gas via the relation $P \propto n^{\gamma+1}$. If we combine the result for the monopole mode frequency for a spherical trap from hydrodynamic theory, equation 4.18, with the result from Tan's Virial Theorem, equation 4.31, it is possible to obtain a formula for the polytropic index. Doing so, one finds that

$$\gamma = \frac{2}{3} + \frac{4}{3}A \tag{4.34}$$

where A is given by equation 4.33. The polytropic index is plotted versus the dimensionless interaction strength $(k_F a)^{-1}$ in Figure 4.7.

Finally, it is also possible to use the contact to derive an expression for the structure factor of our system. The relation 3.4 between Contact and the high momentum tail of the structure factor was derived earlier in Section 3. As the structure factor of a system is an often measured quantity of cold systems, by calculating the Structure for our system at a high momentum, or otherwise at $q >> k_f$, it is possible to introduce a further test of our calculations of the Contact of the system. Using equation 3.4 along with the equation I derived for the Contact I was able to observe the behavior of the structure factor with respect to the dimensionless interaction strength $(k_f a)^{-1}$ at a momentum of $q = 5k_f$. The black line in Figure 4.8 is my calculation, the blue line is a theoretical calculation based on random phase approximation in references [23] and [8], and the filled circles are experimental data from

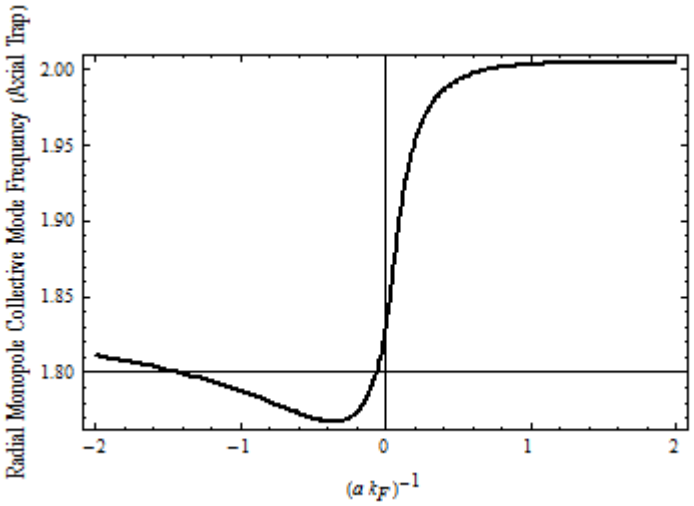

Figure 4.5: Plot of the dimensionless Radial Monopole Collective Mode for an axially symmetric plot ω_+/ω_r versus the dimensionless interaction strength $(k_F a)^{-1}$

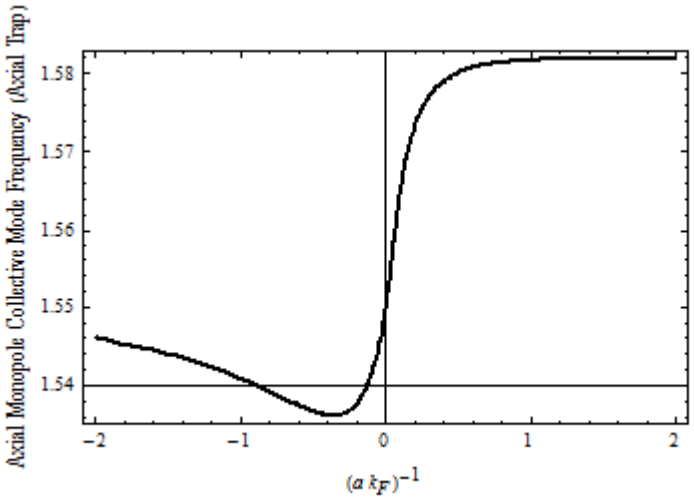

Figure 4.6: Plot of the dimensionless Axial Monopole Collective Mode for an axially symmetric plot ω_a/ω_z versus the dimensionless interaction strength $(k_F a)^{-1}$

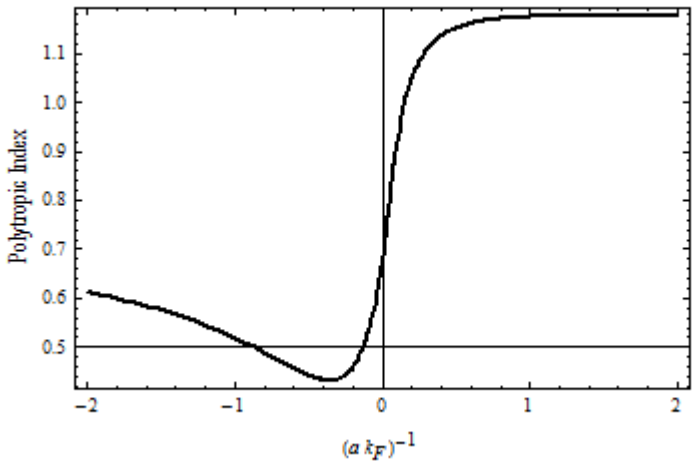

Figure 4.7: Plot of the polytropic index γ versus the dimensionless interaction strength $(k_F a)^{-1}$.

references [23] and [13]. As can be seen from Figure 4.8, my calculation of the structure factor agrees very well with experimental data and an RPA calculation. The only area where is there any discrepancy is at $(k_f a)^{-1} << 1$ which is due to the erroneous behavior of my calculations of Contact in that region, which in section 3.3.2 was attributed to an artifact of the Pade approximation employed in the derivation.

4.2.3 Problems with Sum Rule and Alternative Approaches

Although the results of Section 4.2.2 on the behavior of collective oscillations and the polytropic index of our system predicted by Tan's Contact are accurate in that the sense that they match other theories, computational models, and experimental results, there is a problem with the above derivations. This problem becomes evident when one considers the original virial theorem in equation 4.27 and Tan's virial theorem in equation 3.5 at unitarity. At precisely unitarity where $(k_F a)^{-1} = 0$, it is implied that $a^{-1} = 0$ as $k_F^{-1} = 0$ would imply infinite energy. If this is true then 4.27 and 3.5 together imply

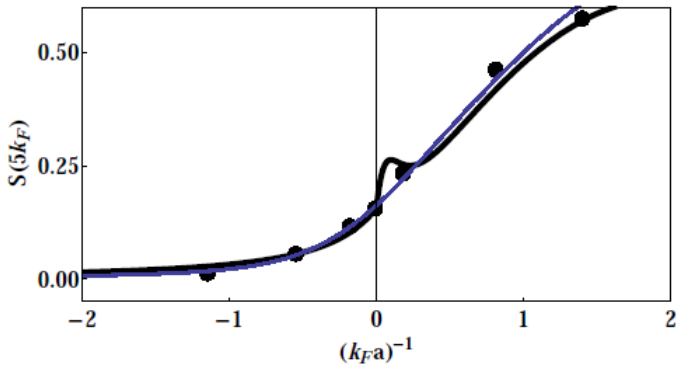

Figure 4.8: Plot of the structure factor S versus dimensionless interaction strength $(k_F a)^{-1}$, the blue line is a theoretical calculation based on random phase approximation in references [23] and [8], and the filled circles are experimental data from references [23] and [13]

that the internal energy $U = 0$, which is obviously not true in a system with strong interactions. The results from these two equations are still correct, as was stated earlier, however, it is very bad practice to use a fundamentally incorrect theory simply because the results are correct. Therefore, I then sought to rederive the above results relating the Contact to the collective oscillations and polytropic index of our system in a framework that avoided the erroneous implication that $U = 0$ at unitarity.

The first step in this new derivation is to rederive a formula for the polytropic index as it is necessary to confirm the result for the collective monopole mode frequencies in an axially symmetric trap and derive the collective monopole and quadrupole frequencies for a spherically symmetric trap. Fortunately, this task was already completed in section 4.1.1 where the polytropic index was given by the equation 4.5. As expected, $\gamma = 2/3$ in the weakly interacting limit $a \to 0^-$ and at unitarity, and $\gamma = 4/3$ in the limit $a \to 0^+$. These limiting values of γ as well as the behavior of the function over the range of values of a when plotted versus $(k_F a)^{-1}$ match the results derived in section 4.2.2. As the result for the polytropic derived in this section exactly matches that derived in section 4.2.2, the results for the behavior of the axial and radial monopole collective mode frequencies in an

axially symmetrical trap exactly match those in section 4.2.2 as well as the mode frequencies are entirely dependent on the polytropic index.

In order to derive the monopole and quadrupole collective mode frequencies for a spherically symmetric trap, I once again use the sum rule over the moments of the response function. This time however, instead of using the relation $\hbar\omega_M = \sqrt{m_3/m_1}$ I use the relation $\hbar\omega_M = \sqrt{m_1/m_{-1}}$. Doing so, I find that

$$\omega_M^2 = \frac{-4\langle r^2\rangle}{md\langle r^2\rangle/db} \tag{4.35}$$

where $b = m\omega_0^2/2$. Writing $\langle r^2\rangle = 4\pi\int_0^{r_0} r^4 n(r)dr$, where $r_0 = \sqrt{\mu_0/b}$ and using $\mu = An^\gamma$, I find that

$$\frac{d\langle r^2\rangle}{db} = -\frac{2\langle r^2\rangle}{b(3\gamma+2)} \tag{4.36}$$

The lowest order breathing mode frequency for spherically symmetric trap is then given by $\omega_M = \sqrt{3\gamma+2}$, which exactly matches the result derived in section 4.2.2. The fact that this new sum rule works for the monopole mode also implies that it works for the quadrupole mode.

Therefore, I have rederived all of the results of section 4.2.2 without the methods which imply that $U = 0$ at unitarity.

4.3 Summary

In conclusion, I used two different methods to derive the Contact for a balanced system of strongly interacting fermions with large scattering length and two different possible spin states. The first method made use of one of Tan's universal relations, the adiabatic sweep theorem (equation 3.6), and a ground state energy functional derived from asymptotic limits and Monte Carlo calculations, and the second method involved a derivation using BCS Mean Field Theory. Both methods produced the same results, although there was a small area of erroneous negative concavity in the result from the first method due to an artifact from the Monte Carlo calculation, and these results matched both a random phase approximation and experimental results. I was also able to calculate the structure factor as a function of dimensionless interaction strength at large values of momentum.

I then used Tan's virial theorems, equations 4.27 and 3.5, to derive the monopole and quadrupole collective mode frequencies for a spherically symmetric trap. The results for the collective modes matched hydrodynamic theory at asymptotic limits as well as at unitarity. I then used hydrodynamic theory generalized to an axially symmetric trap to calculate the axial and radial monopole collective mode frequencies of an axially symmetric trap as a function of the Contact. I was then able to use these results to calculate the polytropic index in terms of the Contact as well.

However, it was found that the approach using equations 4.27 and 3.5 implied that $U = 0$ at unitarity, which is obviously false for a strongly interacting system. Therefore, despite the accuracy of the results, I then used a different approach to rederive all of my results. I first used the Gibbs-Duhem relation to find the chemical potential which I then used to find the polytropic index. I was then able to use the polytropic index along with hydrodynamic theory to rederive the monopole and quadrupole collective modes of a spherically symmetric trap. Finally, I then used a different sum rule to rederive the radial an axial monopole modes of an axially symmetric trap. All the results using this new method matched exactly the results I had already obtained.

Chapter 5

Conclusion

Strongly correlated cold gas systems are extremely interesting systems due to their interesting properties and the large number of experimental methods which allow a great deal of control over the system. Of these systems, those composed of fermions are more interesting still as the Pauli Exclusion Principle allows them further properties not present in Bosonic systems. Unlike bosons, fermions can form bosons through molecular bound states and thus, through a fine degree of control, can be altered to display the traits of both fermionic and bosonic systems.

A great interest in the study of these systems is focused on increasing the degree of control excercised over the system so that further advancements made be made in understanding fundamental physical laws as well as building interesting systems. Therefore, in this project I studied the statics and dynamics of two different fermionic systems in order to advance the understanding and control of these systems.

For my first goal I studied a gas of a single species of fully polarized non-interacting fermions in a quartic trap. I chose to study this system under the influence of a quartic trap as it is common in many experimental setups, such as all gaussian optical traps, and a quartic term helps to stabiliz rapidly rotating gases. The most interesting quantity in this system is the anharmonic term γ in the equation for the potential $V = V(r, z) = br^2 + b_z z^2 + \gamma r^4$ as it determines the strength of the quartic term of the trap and therefore the effect it has upon the trapped gas. I was able to find expressions for the number of particles, total energy, chemical potential, and specific heat of the system. I also plotted the total energy, chemical potential, and specific heat of the system versus the anharmonic term, and plotted the

critical anharmonicity at which the system became unstable as a function of the logarithm of the total number of particles.

My second goal was to extend the usefullness of the recently derived Contact by connecting it to the statics and dynamics of a trapped system. I first defined the Contact to be the high momentum tail of the momentum distribution and then derived several universal realtions associated with it, including expressions for the total energy, the contact density, the structure factor, and a virial theorem. I then applied these universal relations to a balanced strongly interacting gas of fermions with two spin states and large scattering length. The properties of this system allowed me to use the above universal relations to calculate several static and dynamic properties of the gas. The static properties included the total energy, contact density, and polytropic index of the system, and the dynamic properties included the collective oscillations of the trap, the structure factor, and an alternate derivation of the polytropic index. After calculating all the above properties and plotting them with respect to the dimensionless interaction strength $(k_F a)^{-1}$, it was found that they agree well with experimental data and other theoretical models.

Bibliography

[1] M. Bartenstein, A. Altmeyer, S. Riedl, S. Jochim, C. Chin, J. H. Denschlag, and R. Grimm. *Collective Excitations of a Degenerate Gas at the BEC-BCS Crossover. Physical Review Letters*, 92(20), 2004. 203201.

[2] Eric Braaten. volume volume, chapter Chapter: Universal Relations for Fermions with Large Scattering Length. Srpinger, 2011.

[3] V. Bretin, S. Stock, Y. Seurin, and J. Dalibard. *Fast Rotation of a Bose-Einstein Condensate. Physical Review Letters*, 92(5), 2004. 050403.

[4] B. DeMarco, S.B. Pap, and D.S. Jin. *Pauli Blocking of Collisions in Quantum Degenerate Atomic Fermi Gas*, 2001. 865409.

[5] Theja DeSilva. Breathing mode frequencies of a rotating fermi gas in the bcs-bec crossover region. *Physical Reivew A*, 78(2), 2008. 023623.

[6] A. L. Fetter. *Vortices in a Rotating Bose-Einstein Condensate Under Extreme Elongation in a Harmonic Plus Quartic Trap. Physical Review A*, 64(4), 2001. 063608.

[7] Eduardo Fradkin. *Linear Response Theory.* University of Illinois at Urbana-Champaign, 2010. http://webusers.physics.illinois.edu/ efradkin/phys582/LRT.pdf.

[8] X.-J. Liu H. Hu and P. D. Drummond. *Static Structure Factor of a Strongly Correlated Fermi Gas at Large Momenta. Europhysics Letters*, 91(2), 2010. 20005.

[9] H. Heiselberg. *Fermi Systems with Long Scattering Lengths. Physical Review A*, 63(4), 2001. 043606.

[10] Peter Hertel. *Lectures on Theoretical Physics: Linear Response Theory*. University of Osnabruck, Germany, 2011. http://grk.physik.uni-osnabrueck.de/lecture/lrt.pdf.

[11] Y.E. Kim and A.L. Zubarev. *Collective Excitations of Strongly Interacting Fermi Gases of Atoms in a Harmonic Trap. Physical Review A*, 72(1), 2005. 011603.

[12] J. Kinast, S. L. Hemmer, M. E. Gehm, A. Turlapov, and J. E. Thomas. *Evidence for Superfluidity in a Resonantly Interacting Fermi Gas. Physical Review Letters*, 92(15), 2004. 150402.

[13] E. D. Kuhnle, H. Hu, X.-J. Liu, P. Dyke, M. Mark, P. D. Drummond, P. Hannaford, and C. J. Vale. *Universal Behavior of Pair Correlations in a Strongly Interacting Fermi Gas. Physical Review Letters*, 105(7), 2010. 070402.

[14] Austen Lamacraft. Cold atoms for condensed matter theorists. Print.

[15] David Schroeder. An Introduction to Thermal Physics. Addison-Wesley, Reading, Massachusetts, 2000.

[16] J. T. Stewart, J. P. Gaebler, T. E. Drake, and D. S. Jin. *Verification of Universal Relations in a Strongly Interacting Fermi Gas. Physical Review Letters*, 104(23), 2010. 235301.

[17] Shina Tan. Energetics of a strongly correlated fermi gas. *Annals of Physics*, 323(2952-2970), 2008.

[18] Shina Tan. Generalized virial theorem and pressure relation for a strongly correlated fermi gas. *Annals of Physics*, 323(2987-2990), 2008.

[19] Shina Tan. Large momentum part of fermions with large scattering length. *Annals of Physics*, 323(2971-2986), 2008.

[20] K. Xu, T. Muikayamar, J.R. Abo-Shaeer, J.K. Chin, D.E. Miller, and W. Ketterle. *Formation of Quantum-Degenerate Sodium Molecules. Physical Review Letters*, 91(21), 2008. 210402.

[21] J. Yin and Y. Ma. *Analytical Expressions of Collective Excitations for Trapped Superfluid Fermi Gases in a BCS-BEC Crossover. Physical Review A*, 74(1), 2006. 013609.

[22] J. Yin, Y. Ma, and G. Huang. *Frequency Shift and Mode Coupling of the Collective Modes of Superfluid Fermi Gases in the BCS-BEC Crossover. Physical Review A*, 74(1), 2006. 013609.

[23] Peng Zou, Eva D. Kuhnle, Chris J. Vale, and Hui Hu. *Quantitative Comparison Between Theoretical Predictions and Experimental Results for Bragg Spectroscopy of a Strongly Interacting Fermi Superfluid. Physical Review A*, 82(6), 2010. 061605.